# Chemical Nature of Active Sites for Defect-Mediated Nucleation on Silicon Dioxide

**Joseph M. McCrate and John G. Ekerdt**
Dept. of Chemical Engineering, The University of Texas at Austin, Austin, TX 78712

*DOI 10.1002/aic.15023*
*Published online September 14, 2015 in Wiley Online Library (wileyonlinelibrary.com)*

*Germanium nanoparticle growth on $SiO_2$ proceeds via defect-mediated nucleation and particle density can be enhanced by chemically treating the $SiO_2$ with $SiH_x$. The influence of $SiH_x$ fragments on $SiO_2$ surface sites is studied using a fluorescent probe-based technique to understand the chemical nature of the inherent defect trapping sites and the chemical nature of the additional trapping sites formed by $SiH_x$. Oxygen-vacancy sites on $SiO_2$ are the inherent sites for defect-mediated nucleation. $SiH_x$ fragments, generated by cracking disilane on a hot tungsten filament, are shown to react with strained siloxane sites, leading to a conversion of these strained siloxane sites into a different low density defect site that is shown to display reactive characteristics similar to the oxygen-vacancy defect sites. Previous work demonstrating an increased density of Ge nuclei on $SiO_2$ surfaces with increasing $SiH_x$ exposure is interpreted in the context of the current experimental results.* © 2015 American Institute of Chemical Engineers *AIChE J*, 62: 367–372, 2016
*Keywords: nucleation, silicon dioxide, surface defects*

## Introduction

Particle and film formation are governed by several competing phenomena. Nucleation of adatoms generates the initial stable clusters from which particles and films form. Further incorporation of adatoms into a particle causes growth. Particle density decreases through either agglomeration, in which particles merge with their neighbors, or Ostwald ripening, in which smaller particles give up their constituents to larger particles.[1] Semiconductor and metal particles generally grow in a Volmer-Weber, or three-dimensional, growth mode on oxide materials, due to differences between surface and interfacial energies.[1] This means that particles tend to form on these surfaces prior to film formation, so that a continuous film is only obtained when sufficient material has been deposited to cause coalescence of all the particles. Mean-field nucleation and growth rate equations incorporate the concept of a critical cluster size, which is the size such that the addition of one more adatom results in stable nuclei and particle growth proceeds on stable nuclei.[1–5] A critical cluster size of zero is associated with trapping of adatoms on the substrate surface.[6,7] When the densities of these trapping sites are well-below chemically identifiable surface sites, the trapping sites are generally associated with a surface defect.

A number of systems including Fe on Cu(100),[2] metals on MgO[5,8,9] and $TiO_2$,[6,10] and Au on $SiO_2$[11] are known to possess some form of defect-mediated nucleation. A critical cluster size of zero, indicating a single adatom is stable on the surface, has been observed for nucleation of germanium on $SiO_2$[12] and $HfO_2$,[13] suggesting defects may play a role in mediating nucleation in these systems as well.

There is an inherent density of trap sites on $SiO_2$ surfaces ($\sim 10^{11}$ cm$^{-2}$) that serve as nucleation centers for Ge during hot-wire chemical vapor deposition (HWCVD).[14] We have previously demonstrated that the density of Ge nuclei on $SiO_2$ surfaces in HWCVD can be tuned by generating additional surface trap sites on the $SiO_2$ surface.[14] The additional surface trap sites are generated by exposure of $SiO_2$ to $SiH_x$ formed by cracking $Si_2H_6$ over a heated W filament.[14,15] Although we demonstrated the ability to increase the density of Ge nanoparticles deposited using HWCVD by over an order of magnitude (from $\sim 10^{11}$ to $\sim 10^{12}$ cm$^{-2}$) through chemical modification, we were unable to determine the nature of the site or sites responsible for trapping of adatoms that are inherent to $SiO_2$ and that are generated on the $SiO_2$ by $SiH_x$ adsorption. Due to the very low density of the surface sites involved, no traditional surface science experimental techniques were capable of detecting the sites involved in either nucleation process. The lack of a suitable experimental technique for studying such sites motivated us to develop an approach employing fluorescent probe molecules to titrate the possible trap sites at the low densities found for the Ge nanoparticles.

Derivatives of perylene, a high brightness fluorophore, with specific functional groups can be used to titrate various surface

Current address of Joseph M. McCrate: IM Flash Technologies, LLC, 4000 North Flash Drive, Lehi, UT, 84043

Correspondence concerning this article should be addressed to J. G. Ekerdt at ekerdt@utexas.edu.

sites on silica including hydroxyl, strained siloxane,[16] and oxygen-vacancy surface sites[17] with densities of $\sim 1 \times 10^{14}$ $cm^{-2}$ ($1\ nm^{-2}$), $\sim 1 \times 10^{12}$ $cm^{-2}$ ($0.01\ nm^{-2}$), and $\sim 1 \times 10^{11}$ $cm^{-2}$ ($0.001\ nm^{-2}$), respectively. The titration process results in a single fluorescent probe molecule bound to a specific surface site. Performing the entire process in an ultrahigh vacuum (UHV) environment enables the study of surface sites, which may not be stable in ambient conditions. Excitation of the fluorescent molecules using a laser source while the sample is still in a UHV environment enables collection of *in situ* emission spectra. The high sensitivity of such measurements enables detection of molecules, and thus surface sites, with densities below $10^{10}$ $cm^{-2}$.[16,18]

In this work, the fluorescent probe technique is used to explore the chemical nature of the inherent trap sites and the chemical nature of the trap sites resulting from $SiH_x$ fragment exposure, which lead to enhanced Ge nucleation on silica surfaces.[14] The densities of free hydroxyl, strained siloxane, and oxygen-vacancy sites are monitored as a function of $SiH_x$ exposure using the fluorescent probe technique to determine how this $SiH_x$ exposure process alters the surface chemistry of $SiO_2$. Oxygen-vacancy defects (OVDs) are shown to be the likely inherent trap sites on $SiO_2$.

## Material and Methods

Detailed experimental procedures, including the synthesis of fluorescent precursors used in this work, have been described previously.[16–18] Perylene-3-methanol (P3M) and perylene-3-methanamine (P3A) were synthesized[16] and 3-vinyl perylene (3VP) was obtained from the Florida Center for Heterocyclic Compounds. All compounds were purified over a silica gel column and then sublimed onto aluminum foil, which was subsequently loaded into a thermal evaporator cell in the vacuum chamber. The multichamber UHV system used in this work is described elsewhere.[16] This system contains a transfer chamber connected to a load lock, a quartz tube furnace for annealing samples, a chamber for exposing samples to the fluorescent molecules, a chamber with a hot filament for cracking disilane gas, and an analysis chamber containing an x-ray photoelectron spectrometer and a mass spectrometer for temperature programmed desorption (TPD) measurements. The base pressure for all chambers, besides the load lock, was $\sim 1.33 \times 10^{-7}$ Pa.

A 405-nm diode laser with an output power of 20 mW (CrystalLaser) was used as the excitation source for *in situ* emission measurements. An optics assembly connected to the laser via fiber optics was used to focus the beam on the sample with a spot size of $\sim 1\ mm^2$ and collect and transfer emitted light to the spectrometer (Ocean Optics QE6500) via fiber optics. A 425-nm long pass filter was used to eliminate scattered light, and all measurements were collected with 1 s integration times and averaging three spectra.

Cleaned fused silica wafers (Sydor Optics) were loaded onto a Mo sample holder and placed in the load lock.[16] The sample was then transferred to the tube furnace, and annealed at 700°C for 30 min. This step ensures that both free hydroxyl and strained siloxane sites are present on the silica surface.[16] After cooling, samples were moved to a different chamber for exposure to $SiH_x$ fragments.

Cracking of disilane on a hot tungsten filament to generate $SiH_x$ fragments has been described previously.[14,15] The exact nature of the fragments (i.e., $x = 0$, 1, 2, or 3) is unknown. The sample was positioned $\sim$3 cm from a 250 W Osram Xenophot bulb with part of the glass enclosure removed. Disilane gas (4% in He balance, Voltaix) was introduced through a leak valve to bring the partial pressure of disilane to $1.07 \times 10^{-5}$ Pa. The bulb was heated to $\sim 1800\ K$[19] using a 4 A current. The flux of $SiH_x$ fragments was calibrated based on attenuation of the $Si^{4+}$ feature in x-ray photoelectron spectroscopy (XPS) after a 60 min exposure. One monolayer (ML) equivalent was deposited in 3.33 min. For brevity, $SiH_x$ exposure will be subsequently referred to as Si exposure.

After Si exposure, samples were transferred to the analysis chamber and ramped to $\sim$700°C at $\sim$2°C/s. This was performed to replicate the procedure used previously to increase Ge nucleation on $SiO_2$.[14] The nature of this process will be evaluated below.

After cooling to below 100°C, samples were next transferred to a different chamber connected to the UHV system for exposure to the desired fluorescent precursor. The evaporator cell containing the precursor was heated to 60°C for P3A and 3VP precursors and exposure times of 30 min were used for these fluorescent probe molecules.[16,17] The titration of free hydroxyl sites using P3M requires a higher evaporator temperature of 100°C, an exposure time of 60 min, and the addition of a small amount of P3A to catalyze the reaction.[16] Samples were heated to $\sim$80°C for all exposure processes to minimize the amount of physisorbed material.

After exposure to the desired fluorescent probe molecule, samples were transferred to the tube furnace and annealed at 300°C for 30 min to ensure only covalently attached fluorescent molecules remained on the sample surface.[16] After cooling, an *in situ* emission spectrum was collected. This spectrum provides information on the density and proximity of chemically bound fluorophores on the silica surface. Because each type of molecule reacts with certain surface sites, this spectrum thus provides insight into the density and proximity of various surface sites, and is used as the basis of the majority of the following discussion.

## Results and Discussion

Because atomic hydrogen is likely also generated when disilane is cracked on a hot filament to generate $SiH_x$, we briefly review the results of our previous study examining the influence of atomic deuterium exposure on silica surface sites.[17] Atomic deuterium was found not to affect the density of free hydroxyl sites, which is consistent with the literature.[20] Atomic deuterium exposure did not affect the total density of sites that react with P3A; it does chemically transform the strained siloxane sites. However, atomic deuterium exposure did lead to an increase in the density of sites capable of chemisorbing 3VP by cleaving strained siloxane sites and forming ≡Si-D sites, which are likely reactive toward 3VP.[17] Cleavage of strained siloxane (≡Si—O—Si≡) sites by atomic deuterium would form both an ≡Si-D and an ≡Si-OD site. The former site is expected to react with 3VP and also with P3A, while the silanol site is not expected to react with either fluorophore. Therefore, exposure of the $SiO_2$ surface to atomic deuterium leads to an increase in ≡Si-D sites at the expense of strained siloxane sites. As P3A is believed to react with ≡Si-D and strained siloxane and form identical bound structures, no change is observed in the emission spectra between samples with and without atomic deuterium exposure prior to P3A titration. Therefore, only emission spectra from samples titrated with 3VP were affected by atomic deuterium exposure.[17]

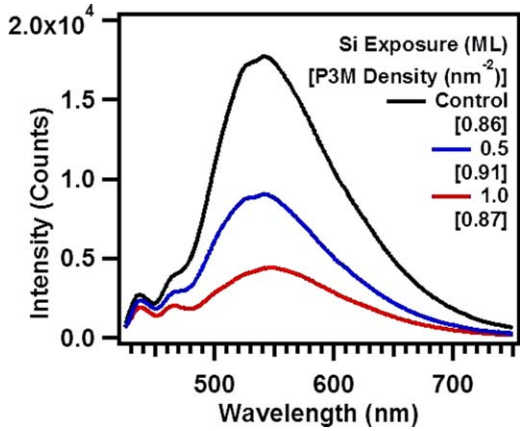


**Figure 1. *In situ* emission intensity from 700°C pretreated samples given various Si exposures and then titrated with P3M.**

**The areal densities in brackets were determined by hydrolytic cleavage of the molecule from the surface.[16] The control sample had no disilane exposure. [Color figure can be viewed in the online issue, which is available at wileyonlinelibrary.com.]**

Figure 1 shows the fluorescence emission intensity from a 700°C-pretreated $SiO_2$ sample given various Si exposures and then titrated with P3M. This molecule is capable of titrating free hydroxyl sites on the silica surface.[16] The broad emission feature observed for all spectra in Figure 1 is characteristic of excimer-like emission due to interaction of adjacent covalently bound perylene fluorophores.[18] For P3M titration, the densities of bound fluorophores can also be determined by hydrolytically cleaving the molecules from the surface into solution, and then measuring the fluorescence emission intensity of the solution and comparing it to standard solutions.[16] This method avoids the complications of the excimer-like emission for high fluorophore coverage (above $\sim$0.1 $nm^{-2}$). The densities determined in this manner are listed in brackets in Figure 1, and show that virtually no change in hydroxyl density is observed with Si exposure.

For the case of P3M titration of hydroxyls, the observed decrease in *in situ* emission intensity is attributed to fluorescence quenching from a bulk defect and not from a decrease in the density of surface hydroxyl sites. Emission intensity was also found to decrease in a similar manner with atomic deuterium exposure, suggesting hydrogen (deuterium) species are responsible for creating the bulk defects. Because of the longer lifetime, the excimer-like species is more susceptible to quenching than the monomer species. This quenching phenomenon is not anticipated to significantly affect the emission from P3A or 3VP-titrated surfaces because the densities are such that monomeric species are observed when they bind to strained siloxane and oxygen vacancy sites, respectively.[16,18]

The impact of the Si exposure on strained siloxane sites can be evaluated using P3A.[16] Figure 2 shows *in situ* emission spectra collected after exposing a 700°C-pretreated silica sample to various Si doses and then titrating with P3A. The control sample was not exposed to disilane gas, while "0 ML" Si exposure was exposed to disilane gas without heating the tungsten filament. With no Si (or disilane) exposure, primarily monomeric emission is observed. Under the control-sample conditions, the density of strained siloxane sites has previously been determined to be $\sim$0.01 $nm^{-2}$ ($10^{12}$ $cm^{-2}$). Exposure to only disilane prior to titration with P3A resulted in a similar spectrum as without any disilane exposure. With 0.1 ML Si exposure, the intensity drops dramatically. At 0.5 ML Si exposure, the much lower intensity is accompanied by a shift to longer wavelengths (excimer-like emission). The excimer-like emission is known to occur from closely spaced perylene moieties,[18] indicating the distribution of fluorophores is not random after Si exposure. At 1.0 ML Si, the emission intensity is nearly below the noise level.

Unlike for the spectra following titration of hydroxyl sites by P3M, which display the decrease in emission intensity due to excimer-like quenching, the decrease in emission intensity from the covalently attached P3A molecules is attributed to a decrease in strained siloxane sites. Due to the shorter lifetime of the monomeric species relative to the excimer-like species,[17,18] quenching of the monomeric emission intensity for 0.1 ML Si exposure is not anticipated to be as significant as the excimer-like emission that dominates P3M emission. Additionally, quenching would not explain the change in the shape of the emission profile observed with increasing Si exposure to 0.5 ML. We have previously reported atomic deuterium exposure did not result in a dramatic change to the emission intensity from P3A-titrated silica surfaces.[17] The combination of observations indicates the $SiH_x$ fragments are interacting with the strained siloxane sites, forming new sites incapable of chemisorbing P3A.

A vinyl derivative of perylene, 3VP, was previously shown to titrate ultralow density ($\sim$0.001 $nm^{-2}$) surface sites on silica, which were suggested to be OVDs.[17] Figure 3 shows spectra collected from silica surfaces exposed to specific Si doses and subsequently titrated with 3VP. Emission from a sample with no Si exposure ("None" in Figure 3) has previously been estimated to correspond to approximately $10^{11}$ sites/$cm^2$ ($\sim$0.001 $nm^{-2}$). For low Si exposures (0.1 ML), the intensity increases by approximately one order of magnitude, with a broad tail indicative of some excimer-like emission from closely spaced fluorophores.[18] This suggests the density of sites capable of reacting with 3VP increased to approximately $10^{12}$ $cm^{-2}$, although the exact densities are difficult to estimate due to the combination of monomeric and excimer-

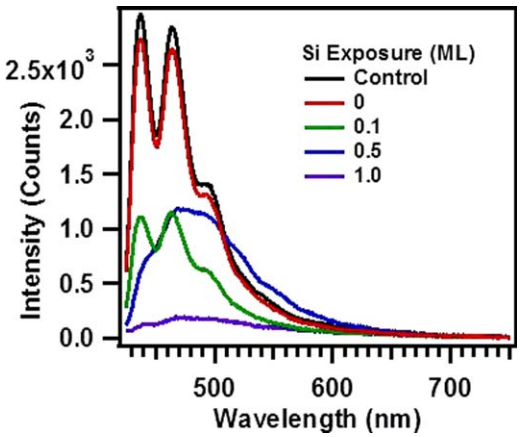


**Figure 2. *In situ* emission intensity from 700°C pretreated samples given various Si exposures and then titrated with P3A.**

**The control sample had no disilane exposure, while "0 ML" was exposed to disilane in the absence of a hot tungsten filament. [Color figure can be viewed in the online issue, which is available at wileyonlinelibrary.com.]**

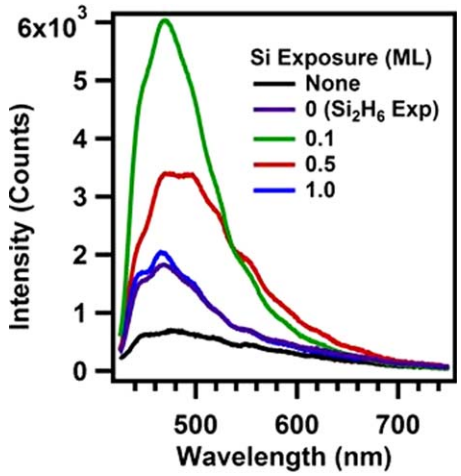


**Figure 3. Emission spectra from 700°C pretreated silica samples given various Si exposures and subsequently titrated with 3VP.**

**Note: "None" means that the sample was not exposed to any disilane, while "0 ML" indicates the sample was exposed to disilane gas in the absence of a hot tungsten filament. [Color figure can be viewed in the online issue, which is available at wileyonlinelibrary.com.]**

like emission for the 0.1 ML exposure.[18] For 0.5 ML Si exposure, the intensity decreases to nearly half of the 0.1 ML peak and is predominantly excimer-like, indicating more perylene fluorophores are in close proximity to each other. As noted above, due to energy migration from monomeric species to excimer-like species, the relative monomeric and excimer-like components of emission do not directly correspond to the relative fractions of each type of species on the silica surface.[18] Emission intensity decreases further at 1.0 ML Si exposure; however, unlike for P3A, a peak is still clearly visible. Emission from a sample exposed only to disilane gas (i.e., the filament was not heated) has a similar intensity as the 1.0 ML Si exposure sample. This indicates that disilane itself may react to some extent with the silica surface, as discussed further below.

The observed increase in emission intensity at low (0.1 ML) Si exposures compared with no exposure indicates Si exposure

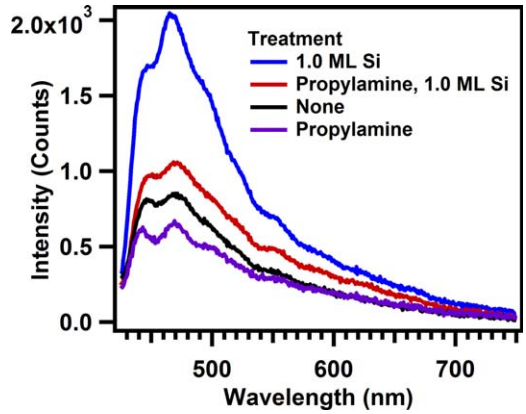


**Figure 4. Emission spectra from a 700°C pretreated silica sample given the specified treatment prior to titration with 3VP.**

**[Color figure can be viewed in the online issue, which is available at wileyonlinelibrary.com.]**

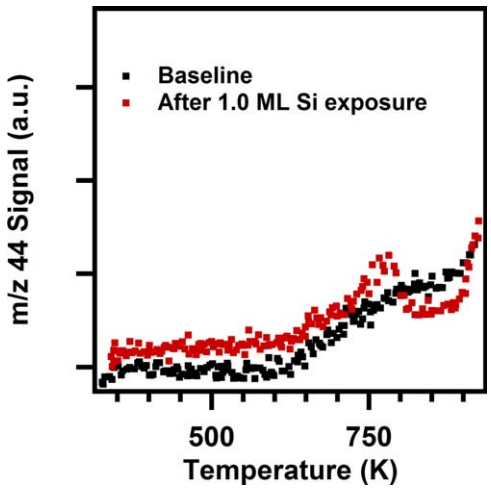


**Figure 5. TPD spectra of *m/z* 44 from thermal oxide on Si(100) before and after exposure to 1.0 ML Si.**

**[Color figure can be viewed in the online issue, which is available at wileyonlinelibrary.com.]**

leads to the formation of additional surface sites capable of reacting with the 3VP. The presence of excimer-like emission after 0.1 ML Si exposure indicates some fraction of the fluorophores is in close proximity. The decrease in intensity and shift to predominantly excimer-like emission with increasing (0.5 and 1.0 ML) Si exposures could be explained by generation of additional sites reactive toward 3VP, with each bound fluorophore in close proximity to another. Additionally, a decrease in emission intensity could be due to an interaction between the site formed by Si exposure and additional $SiH_x$ fragments, forming a new site incapable of binding 3VP.

One possible explanation for the decreased P3A emission intensity at low (0.1 ML) Si exposure (Figure 2) and the increased 3VP emission intensity (Figure 3) is that strained siloxane sites are converted to sites reactive toward 3VP by the Si exposure process. This hypothesis was tested by reacting the strained siloxane sites with *n*-propylamine to eliminate them prior to the Si exposure process. *n*-Propylamine has previously been shown to eliminate strained siloxane sites by forming a Si-NH-R structure.[16,21,22] Spectra from this sample and related treatments are shown in Figure 4. Exposure to *n*-

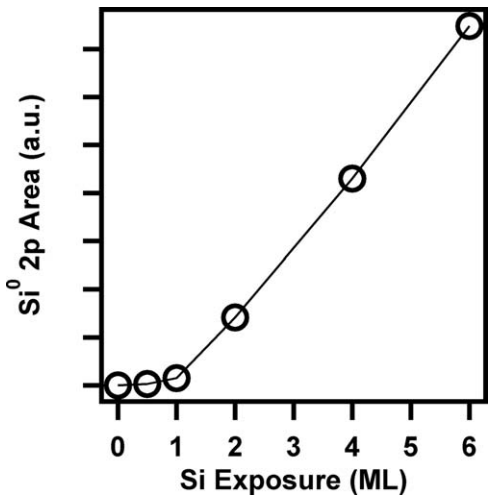


**Figure 6. Plot of $Si^0$ 2p area vs. Si exposure.**

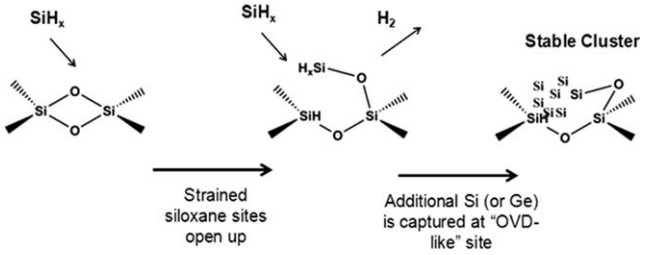


**Figure 7. Proposed mechanism for the interaction of $SiH_x$ fragments with strained siloxane sites.**

**The sites formed through this process appear capable of trapping adatoms, leading to increased nuclei density.**

propylamine prior to 1.0 ML Si exposure results in an emission spectrum that is similar in intensity and shape to a sample without Si exposure. Exposure to only *n*-propylamine prior to titration with 3VP also results in a similar spectrum to the untreated sample, indicating *n*-propylamine does not react readily with the sites capable of chemisorbing 3VP. These results reinforce the interpretation that strained siloxane sites are converted by the Si exposure process to sites capable of chemisorbing 3VP.

Strained siloxane sites also appear capable of reacting directly with disilane, explaining the emission intensity increase in Figure 3 with only a disilane exposure (no hot filament) prior to titration with 3VP. This is consistent with other reports, which found silane compounds reacted slowly with strained siloxane sites.[23]

Based on the preceding results, the Si exposure process clearly affects the chemical nature of the silica surface. Previous work examining the nature of the Si exposure process on $SiO_2$ found evidence of a $m/z-44$ signal in TPD measurements, suggesting the formation of volatile SiO.[15] The formation of SiO from the reaction of Si and $SiO_2$ is known to occur under certain circumstances,[23] leading us to suggest that the $SiH_x$ fragments were etching the silica surface.[15] We re-evaluated this hypothesis by performing similar TPD measurements, but used a Si-coated sample holder to eliminate contributions from the sample holder to the TPD signal. We were unable to reproduce earlier spectra with this different sample holder. Figure 5 shows the TPD spectra for $m/z-44$ collected from thermal oxide on Si(100) with and without a 1.0 ML Si exposure. Only a very weak feature is observed around 750 K. The previous observation of a $m/z-44$ signal that was attributed to $SiO^+$ is instead likely due to $CO_2^+$, which could result from carbon contamination on the Mo sample holder. Hence, the Si exposure process does not lead to etching the $SiO_2$ surface.

In addition to TPD measurements, XPS was used to gain insight into the Si exposure process. Figure 6 shows the plot of $Si^0$ 2p area vs. Si exposure. For exposures below 1.0 ML, only very weak $Si^0$ features are observed. At higher exposures, the peak area, and hence amount of deposited material, increases linearly with exposure. The plot shows two distinct regions: an early induction period followed by Si deposition. As discussed below, Si exposure in the early induction period appears to alter the surface chemistry of $SiO_2$ in such a manner that it supports subsequent nucleation.

The Si exposure process affects the densities of the strained siloxane and oxygen vacancy sites differently than atomic deuterium exposure. Sites that react with 3VP in a chemically similar manner to oxygen-vacancy sites appear to increase in density at the expense of strained siloxane sites following Si exposure. Further, the presence of excimer-like emission from both P3A and 3VP-titrated surfaces after Si exposure (Figures 2 and 3) indicates fluorophores are bound in close proximity to each other,[18] and not randomly distributed on the surface. This latter observation is important, because atomic deuterium exposure did not result in similar excimer-like emission.

This same Si exposure process has previously been shown to lead to increased density of Ge nanoparticles from HWCVD.[14] HWCVD was used because conventional thermal CVD is not capable of nucleating Ge particles directly on $SiO_2$.[24–26] The increased nuclei density was attributed to the formation of sites capable of trapping Ge adatoms.[14] Notably, the density of Ge nanoparticles increased from $\sim 10^{11}$ $cm^{-2}$ ($0.001$ $nm^{-2}$) with no Si exposure to $\sim 10^{12}$ $cm^{-2}$ ($0.01$ $nm^{-2}$) with 1.0 ML Si exposure, which corresponds to roughly the same densities of the sites that react with 3VP with no Si exposure (OVD sites) and after Si exposure. The observed Ge nanoparticle densities were presumed to be the saturation densities for the specified Si exposures. The correlation between Ge nuclei density and oxygen vacancy sites (i.e., reactive toward 3VP) in the absence of Si exposure suggests that oxygen-vacancy sites are the inherent trap sites on $SiO_2$ for Ge adatoms. The increase in Ge nucleation density and bound 3VP with increasing Si exposures up to 1 ML further supports the interpretation that oxygen-vacancy like sites are generated by Si exposure and serve as additional trap sites for Ge adatoms. Therefore, OVD sites appear to control Ge nuclei density during HWCVD of $GeH_4$ on $SiO_2$ both intrinsically and as a result of chemical modification through the Si exposure process.

We propose the mechanism depicted in Figure 7 for explaining the observations from the titration experiments reported in this work and the enhanced Ge nucleation with increasing Si exposure reported previously.[14] $SiH_x$ fragments react with strained siloxane sites, opening up the structure and forming $\equiv$SiH and $-SiH_x$ sites in close proximity to each other. Both of these sites are likely capable of reacting with 3VP, explaining the increase in emission intensity from samples given Si exposures and titrated with 3VP (Figure 3). After additional Si exposure, such structures may then serve as the trap sites capable of capturing additional Si or Ge adatoms and leading to particle nucleation. The conversion of strained siloxane sites to sites capable of trapping adatoms explains the increase in Ge nuclei density with increasing Si exposure. This model suggests that ultralow density sites, which are not readily detectable using traditional surface science techniques, play a key role in nucleation processes on the silica surface.

## Conclusions

The interaction of $SiH_x$ fragments with various low density surface sites on the amorphous silica surface has been studied using a fluorescent probe technique. Perylene derivatives with specific functional groups were used to titrate free hydroxyl and strained siloxane sites, as well as sites that are most likely oxygen vacancies. Exposure of the silica surface to $SiH_x$ fragments does not appear to impact the density of free hydroxyl sites. However, strained siloxane sites appear to be converted to adjacent oxygen vacancy-like sites during the Si exposure process. The density of the oxygen vacancy and oxygen vacancy-like sites ranges from approximately $10^{11}$ sites/$cm^2$ ($0.001$ $nm^{-2}$) with no Si exposure to over $10^{12}$ sites/$cm^2$ ($0.01$ $nm^{-2}$) with one ML of Si exposure. These densities are in agreement with the densities of Ge nanoparticles observed in our previous work examining the influence of the Si

exposure process on nucleation, indicating the oxygen-vacancy sites are likely the sites responsible for Ge adatom capture. This work sheds light on the relationship between ultralow density surface sites, which are detectable by titration with fluorescent probes, and nucleation. Further studies on the chemical nature of these ultralow density surface sites may provide additional insight into important phenomena, including catalysis and nucleation of other material systems.

## Acknowledgment

This work was supported by the Robert A. Welch Foundation (Grant No. F-1502) and the National Science Foundation (Award CBET-1160195).

## Literature Cited

1. Ratsch C, Venables J. Nucleation theory and the early stages of thin film growth. *J Vac Sci Technol*. 2003;21(5):S96–S109.
2. Chambliss DD, Johnson KE. Nucleation with a critical cluster size of zero: submonolayer Fe inclusions in Cu(100). *Phys Rev B*. 1994; 50(7):5012–5016.
3. Amar JG, Family F. Critical cluster size: island morphology and size distribution in submonolayer epitaxial growth. *Phys Rev Lett*. 1995; 74(11):2066–2069.
4. Kandel D. Initial stages of thin film growth in the presence of island-edge barriers. *Phys Rev Lett*. 1997;78(3):499–502.
5. Venables JA, Giordano L, Harding JH. Nucleation and growth on defect sites: experiment–theory comparison for Pd/MgO(001). *J Phys Condens Matter*. 2006;18:S411–S427.
6. Zhou J, Chen DA. Controlling size distributions of copper islands grown on $TiO_2$(110)-(1 × 2). *Surf Sci*. 2003;527:183–197.
7. Wedding JB, Wang G-C, Lu T-M. Vacancy-enhanced submonolayer nucleation of Si on Si(111). *Surf Sci*. 2002;504:28–36.
8. Haas G, Menck A, Brune H, Barth JV, Venables JA, Kern K. Detection of low-density surface sites on silica: experimental evidence of intrinsic oxygen-vacancy defects. *Phys Rev B*. 2000;61(16):11105–11108.
9. Bogicevic A, Jennison D. Effect of oxide vacancies on metal island nucleation. *Surf Sci Lett*. 2002;515(2–3):L481–L486.
10. Wahlström E, Lopez N, Schaub R, Thostrup P, Rønnau A, Africh C, Lægsgaard E, Nørskov JK, Besenbacher F. Bonding of gold nanoclusters to oxygen vacancies on rutile $TiO_2$(110). *Phys Rev Lett*. 2003;90(2):026101.
11. Min BK, Wallace WT, Santra AK, Goodman DW. Role of defects in the nucleation and growth of Au nanoclusters on $SiO_2$ thin films. *J Phys Chem B*. 2004;108(42):16339–16343.
12. Li Q, Krauss JL, Hersee S, Han SM. Probing interactions of Ge with chemical and thermal $SiO_2$ to understand selective growth of Ge on Si during molecular beam epitaxy. *J Phys Chem C*. 2007;111(2): 779–786.
13. Coffee SC, Ekerdt JG. Investigation of Volmer-Weber growth mode kinetics for germanium nanoparticles on hafnia. *J Appl Phys*. 2007; 102:114912.
14. McCrate JM, Salivati N, Ekerdt JG. Hot-wire CVD of Ge nanoparticles on Si-etched silicon dioxide. *J Cryst Growth*. 2011;321(1): 131–135.
15. Winkenwerder WA, Ekerdt JG. Interaction of germanium with silicon dioxide. *Surf Sci*. 2008;602(16):2796–2800.
16. McCrate JM, Ekerdt JG. Titration of free hydroxyl and strained siloxane sites on silicon dioxide with fluorescent probes. *Langmuir*. 2013;29:11868–11875.
17. McCrate JM, Ekerdt JG. Detection of low-density surface sites on silica: experimental evidence of intrinsic oxygen-vacancy defects. *Chem Mater*. 2014;26:2166–2171.
18. McCrate JM, Ekerdt JG. Coverage-dependent luminescence from two-dimensional systems of covalently attached perylene fluorophores on silica. *J Phys Chem C*. 2014;118:2104–2114.
19. Coffee SC, Shahrjerdi D, Banerjee SK, Ekerdt JG. Selective silicon nanoparticle growth on high-density arrays of silicon nitride. *J Cryst Growth*. 2007;308(2):269–277.
20. Finlayson-Pitts BJ. Interaction of gas-phase deuterium atoms with silica surfaces. *J Phys Chem*. 1982;86(18):3499–3501.
21. Morrow BA, Cody IA. Infrared studies of reactions on oxide surfaces. 5. Lewis acid sites on dehydroxylated silica. *J Phys Chem*. 1976;80(18):1995–1998.
22. Bunker BC, Haaland DM, Michalske TA, Smith WL. Kinetics of dissociative chemisorption on strained edge-shared surface defects on dehydroxylated silica. *Surf Sci*. 1989;222(1):95–118.
23. Streit DC, Allen FG. Thermal and Si-beam assisted desorption of $SiO_2$ from silicon in ultrahigh vacuum. *J Appl Phys*. 1987;61(8): 2894–2897.
24. Halbwax M, Renard C, Cammilleri D, Yam V, Fossard F, Bouchier D, Zheng Y, Rzepka E. Epitaxial growth of Ge on a thin $SiO_2$ layer by ultrahigh vacuum chemical vapor deposition. *J Cryst Growth*. 2007;308:26–29.
25. Stanley SK, Joshi SV, Banerjee SK, Ekerdt JG. Surface reactions and kinetically-driven patterning scheme for selective deposition of Si and Ge nanoparticle arrays on $HfO_2$. *Surf Sci Lett*. 2006;600: L54–L57.
26. Stanley SK, Joshi SV, Banerjee SK, Ekerdt JG. Ge interactions on $HfO_2$ surfaces and kinetically driven patterning of Ge nanocrystals on $HfO_2$. *J Vac Sci Technol A*. 2006;24(1):78–83.

*Manuscript received June 24, 2015, and revision received Aug. 24, 2015.*